Niobium(V) Oxido Tris-Carbamate as Easily Available and Robust Catalytic Precursor for the Selective Sulfide to Sulfone Oxidation

Giulio Bresciani,[a,b] Mario Gemmiti,[c] Gianluca Ciancaleoni,[a,b,*] Guido Pampaloni,[a,b] Fabio Marchetti,[a,b,*] Marcello Crucianelli[c,*]

[a]*Dipartimento di Chimica e Chimica Industriale, University of Pisa, Via G. Moruzzi 13, I-56124 Pisa, Italy.*

[b]*CIRCC, via Celso Ulpiani 27, I-70126 Bari, Italy.*

[c]*Dipartimento di Scienze Fisiche e Chimiche, University of L'Aquila, Via Vetoio, I-67100 L'Aquila, Italy.*

Abstract

The oxidation of the sulfide function promoted by a variety of vanadium compounds has been largely explored, whereas the use of homogeneous catalytic systems based on the heavier group 5 metals remains less explored. We report the use of easily available niobium and tantalum carbamates, i.e. $[M(O_2CNMe_2)_5]$ (M = Nb, **1**; M = Ta, **2**), $[Nb(O_2CNMe_2)_4]$, **3**, $[NbO(O_2CNEt_2)_3]$, **4**, and $[NbCl_3(O_2CNEt_2)_2]$, **5**, as effective catalysts for the conversion of a series of alkyl aryl and aromatic sulfides into the corresponding sulfones. NMR investigations on the performant niobium catalyst **4** unexpectedly revealed the substantial stability of this compound in the protic catalytic environment, and a plausible catalytic cycle was obtained by DFT studies. The two active catalytic species, *i.e.* **4** and its minor mono-methoxide derivative, presumably interconvert to each other exploiting the versatile coordination of the carbamato ligand.

Keywords: homogeneous catalysis; sulfide oxidation; hydrogen peroxide; niobium and tantalum; metal carbamates.

1. Introduction

The selective oxidation of organic sulfides represents an important chemical transformation due to both the practical utility of sulfoxides and sulfones as high-value commodity chemicals and green chemistry issues (*e.g.*, the oxidative desulfurization of fuels to remove benzothiophene derivatives). Indeed, sulfoxides and sulfones are versatile synthons which are incorporated in a variety of chemically and biologically active molecules, including chiral auxiliaries, drugs and agrochemicals [1]. In addition, a significant application is the selective detoxification of organosulfide-containing chemical warfare agents, wherein a high selectivity to the less toxic sulfoxide product is critical [2]. In the past, several

promising catalytic strategies for selective sulfur oxidation, using various oxidants, have been developed based on transition metal catalysts, particularly those from groups 4–7, in their highest oxidation states [3]. In this frame, many vanadium complexes in +V and +IV oxidation states have been employed as catalytic precursors for sulfide oxidation [4]. With reference to the heavier group 5 elements, high valent niobium- and tantalum-based catalytic systems have found significant applications in several metal-directed organic transformations exploiting the Lewis acidic character of the metal centre [5]. Nevertheless, the use of niobium and tantalum species in homogeneous catalytic oxidation reactions has been significantly less developed [5a,6], and only few works have appeared in the literature regarding the oxidation of sulfur functions [7,8,9]. However, the great interest in exploiting the catalytic potential of niobium and tantalum compounds has increasingly aroused the attention of several researchers [5c,10]. Studies in this field are further encouraged by the substantial nontoxicity of niobium and tantalum as elements [11]. Regarding the current ecological concerns, the quest for safe oxidation processes employing benign solvent, green oxidants and reagents, thus affording harmless by-products, is growing fast. Within the multitude of available organic oxidants, H_2O_2 has been recognized as the best waste-preventing and atom-efficient one, producing water as the only side product, featured by high oxygen content, low cost, safety and easy handling [12].

Metal *N*,*N*-dialkylcarbamates, $[M(O_2CNR_2)_n]$ (R = alkyl group), constitute a class of simple compounds accessible for a wide number of elements throughout the periodic table, from metal halide precursors (usually chlorides) by one-pot CO_2 fixation at atmospheric pressure in the presence of dialkylamines (Eq. 1) [13].

$$MX_n + n\,CO_2 + 2n\,NHR_2 \rightarrow [M(O_2CNR_2)_n] + n\,(NH_2R_2)X \qquad (1)$$

The peculiar features of the carbamato ligand, i.e. the easy availability from commercial chemicals, the adaptability to both bi- and monodentate coordination modes, and the possible dissociation from the

metal coordination sphere in the presence of acidic species through favourable CO_2 release, render metal carbamates intriguing candidates to play as homogeneous catalysts in organic synthesis. On the other hand, the general instability towards moisture and the reactivity towards protic solvents of the carbamato ligand, especially when coordinated to oxophilic metal centers, has limited the studies on the possible applications of metal carbamates [14,38a]. Notwithstanding, working under anhydrous conditions, a range of metal carbamates have been successfully investigated in the H_2 hydrogenation of 1-octene [15], the polymerization of alkenes [5b,16], the polymerization of cyclic esters [17], and also the synthesis of small valuable molecules exploiting CO_2-activation routes [18, 19]. In a number of cases, it has been found that mixed metal halide-carbamates perform better than the respective homoleptic counterparts [18b,19,20]. Targeted syntheses of such hybrid compounds have been reported for titanium(IV), zirconium(IV) and hafnium(IV), via metathesis reactions of the homoleptic metal carbamates with either the corresponding metal chlorides or sodium/ammonium salts [16b,21]. In this setting, the use of metal carbamates as promoters of oxidation reactions has not been explored heretofore: herein, we report a study on the use of a series of high valent niobium and tantalum carbamates, including non-homoleptic species containing oxido or chlorido co-ligands, in the H_2O_2-promoted mild and selective oxidation of a variety of sulfide substrates.

2. Experimental section

General details. Reactants and solvents were commercial products (Merck, TCI Europe or Strem) of the highest purity available, and stored under N_2 as received. Commercially available aqueous solution of H_2O_2 were used after iodometric titration (9.6 ± 0.2 M H_2O_2 in water). IR spectra (650-4000 cm^{-1}) were recorded on a Perkin Elmer Spectrum One FT-IR spectrometer, equipped with a UATR sampling accessory. IR spectra of solutions were recorded on a PerkinElmer Spectrum 100 FT-IR spectrometer with a CaF_2 liquid transmission cell (2000−1200 cm^{-1} range). NMR spectra were recorded at 298 K with a Bruker Avance II DRX 400 instrument equipped with a BBFO broadband probe. Chemical shifts for

^{1}H and ^{13}C were referenced to the non-deuterated aliquot of the solvent [22]. CHN analyses were performed on a Vario MICRO cube instrument (Elementar). ESI-MS spectra were recorded on Waters Xevo © G2 instrument with electrospray ionization (ESI) and detection of positive ions. Sample concentration of 1mg/mL was prepared in methanol. Analysis was carried out under the following conditions: flow 0.02 mL/min, desolvation temperature 200 °C, source temperature 150 °C, drying-gas flow 13 L/min, voltage 6000 V and target mass from 50 to 1200. Gas chromatographic (GC) analyses were performed by means of a ThermoFischer Trace 1300 series instrument equipped with a mass spectrometer (MS) ThermoFischer ISQ 4000 (230 V) detector, using a J&W HP-5 30 m × 0.32 mm × 0.25 μm film thickness fused silica column and chromatography grade helium, as carrier gas (1.5 mL/min.). The injection volume was 1.0 μL. The temperatures of the GC system were the following: injector temperature 250 °C; transfer line temperature 280 °C; oven temperature program: 72 °C (1.0 min.); then, 20°C/min. till 180°C; then, 10°C/min. till 230 °C; lastly, 5°C/min. till 250 °C (5.0 min.). MS detector (quadrupole) was operated in the EI mode at 70 eV, with a mass scan range of 35–350 m/z.

2.1 Synthesis and characterization of metal compounds

Operations were conducted under N_2 atmosphere using standard Schlenk techniques; the reaction vessels were oven dried at 140 °C prior to use, evacuated (10^{-2} mmHg) and then filled with N_2. Compounds **1-3** [23], **4** [24] and **5** [19] were prepared according to the respective literature procedures.

2.2 Catalytic reactions

General procedure. 0.5 mmol of sulfide and 1.0 mL of solvent (methanol or acetonitrile) were introduced into a 3 mL vial, then dinitrogen was fluxed for ca. 3 minutes. Then, while keeping the vial under a cone under N_2 flux, the catalyst (1.0 mol %) and the appropriate amount (2.0 or 3.0 equiv.) of 30% aqueous solution of hydrogen peroxide were added to the mixture. The sealed vial was either thermostated at 45 °C through an oil bath or left at room temperature, under stirring. After 1.5 or 2.0 h (in relation to the

substrate), additional equivalent of oxidant was added dropwise when necessary. At the end of the reaction, the mixture was treated with 5.0 mg of MnO_2 to quench the excess of oxidant and, after 10 minutes, filtered. The progress of the reaction was monitored through GC-FID analysis, by withdrawing an aliquot of 20 μL and adding 5 μL of *n*-hexadecane (internal standard). The oxidation products were identified by comparison of their GC retention times with those of authentic samples.

2.3 Spectroscopic studies

a) NMR and IR spectra of **4**: ^{1}H NMR (toluene-d^{8}): δ/ppm = 3.03 (m, 2H, CH_2); 0.86 (m, 3H, CH_3). $^{13}C\{^{1}H\}$ NMR (toluene-d^{8}): δ/ppm = 162.0, 168.1 (C=O); 39.5, 41.7 (CH_2); 12.1, 13.1 (CH_3). ^{1}H NMR (CD_3OD): δ/ppm = 3.03 (q, 2H, $^{3}J_{HH}$ = 7.2 Hz, CH_2); 1.31 (t, 3H, $^{3}J_{HH}$ = 7.0 Hz, CH_3). $^{13}C\{^{1}H\}$ NMR (CD_3OD): δ/ppm = 161.4 (C=O); 43.5 (CH_2); 12.0 (CH_3). IR (CD_3OD, ν/cm^{-1}) = 1667s-sh, 1626vs (C=O), 1528m, 1507w-sh, 1478vw, 1458m, 1438vw, 1400w, 1391w, 1377w, 1339s, 1255w. IR (solid state, ν/cm^{-1}) = 2974w, 2935w, 2876w, 1620m, 1576s (C=O), 1558s (C=O), 1484m, 1433vs, 1380m, 1321s, 1301s, 1209m, 1100w–m, 1074m, 1022 w, 977w-m, 929vs, 840s, 782s.

b) In a Schlenk tube, a solution of **4** (98 mg, 0.21 mmol) in CD_3OD (2 mL) was treated with a solution of H_2O_2 in water (71.4 μL, 1.26 mmol). After 6 hours, NMR analysis revealed the formation of a minor amount of N-ethylideneethanamine oxide, displaying signals as follows. ^{1}H NMR (CD_3OD): δ/ppm = 7.27 (m, 1H, CH); 3.87 (q, 2H, $^{3}J_{HH}$ = 6.8 Hz, CH_2); 2.00 (m, 3H, CH_3); 1.42 (t, 3H, $^{3}J_{HH}$ = 7.3 Hz, CH_3). $^{13}C\{^{1}H\}$ NMR (CD_3OD): δ/ppm = 141.1 (CH); 60.4 (CH_2); 13.5 (CH_3); 13.0 (CH_3). **4** : N-ethylideneethanamine oxide ratio = 6. The ratio did not substantially vary after 20 hours or when a large excess of H_2O_2 (50÷150 eq.) was used. The IR spectrum after 6 hours was as follow. IR (CD_3OD, ν/cm^{-1}) = 1666m-sh, 1626vs (C=O), 1527vw, 1476w-m, 1457m, 1415w-sh, 1398m, 1378w-sh, 1339vs, 1261vw, 1222w.

c) In a Schlenk tube, a solution of **4** (84 mg, 0.18 mmol) in CD_3OD (2 mL) was treated with Me_2S (65.8 µL, 0.90 mmol). The resulting mixture was stirred for 20 hours at room temperature and then analysed by NMR. ^1H NMR (CD_3OD): δ/ppm = 2.09 (s, 6H, Me) ppm. Then a solution of H_2O_2 in water (180 µL, 3.18 mmol) was added. The system was stirred for 20 hours at room temperature and then analysed by NMR revealing the almost quantitative formation of Me_2SO_2. ^1H NMR (CD_3OD): δ/ppm = 3.01 (s, 6H, Me).

d) In a Schlenk tube, a solution of **4** (84 mg, 0.18 mmol) in CD_3OD (2 mL) was treated with Me_2SO (63.9 µL, 0.90 mmol). The resulting mixture was stirred for 20 hours at room temperature and then analysed by NMR. ^1H NMR (CD_3OD): δ/ppm = 2.67 (s, 6H, Me).

e) In a round bottom flask, a solution of H_2O_2 in water (357 µL, 6.30 mmol) was mixed to a solution of Me_2S (132 µL, 1.80 mmol) in CD_3OD (2 mL). The mixture was stirred for 20 hours and then analysed by NMR. Almost quantitative formation of Me_2SO was detected.

2.4 Theoretical studies

All geometries were optimized with ORCA 4.1.0 [25], using the BP86 functional in conjunction with a triple-ζ quality basis set (ZORA-TZVP) and def2/J auxiliary basis. Relativistic effects were accounted by using the Zeroth Order Regular Approximation (ZORA) scalar correction. The dispersion corrections were introduced using the Grimme D3-parametrized correction and the Becke−Johnson damping to the DFT energy [26]. The polarity of the solvent was taken into account by using the conductor-like polarizable continumm (CPCM) model, as implemented in ORCA 4.1.0 (methanol). All the structures were confirmed to be local energy minima (no imaginary frequencies for intermediates, one imaginary frequency describing the reaction coordinate for TSs).

3. Results and discussion

The catalysts investigated in the present work were synthesized according to the literature. Figure 1 gives a comparative view of the previously described solid-state structures of these catalysts. Thus, **1** and **2** are isostructural mononuclear complexes comprising three bidentate and two monodentate carbamates coordinated to the M^V centre; **3** consists of four equivalent bidentate carbamates bound to Nb^{IV}; **4** is a dimer wherein each Nb^V is coordinated to one terminal oxido ligand, two terminal and two bridging coordinated bidentate carbamato moieties; **5** presents a pentagonal bipyramidal geometry with the two bidentate carbamato ligands occupying the equatorial positions around the Nb^V.

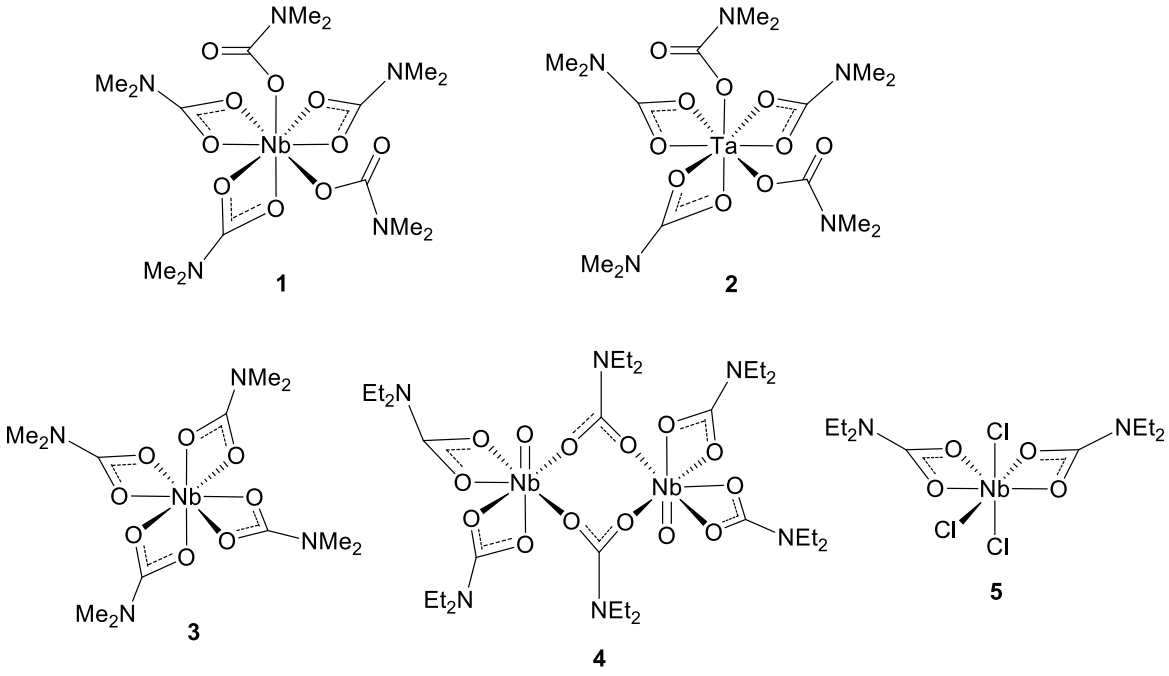

Figure 1. Structures of complexes employed in the present catalytic study: $[Nb(O_2CNMe_2)_5]$, **1** [**Error! Bookmark not defined.**]; $[Ta(O_2CNMe_2)_5]$, **2** [**Error! Bookmark not defined.**]; $[Nb(O_2CNMe_2)_4]$, **3** [**Error! Bookmark not defined.**]; $[NbO(O_2CNEt_2)_3]_2$, **4** [**Error! Bookmark not defined.**]; $[NbCl_3(O_2CNEt_2)_2]$, **5** [19].

3.1 Oxidation of methyl aryl sulfides to the corresponding sulfones.

In this study, our main goal was to evaluate the catalytic power of the metal carbamates **1-5** in promoting the oxidation of a selection of methyl aryl sulfides up to the corresponding sulfones, under mild conditions and using hydrogen peroxide as oxidant (Scheme 1). Thus, the performance of **1-5** was initially screened in the H_2O_2 promoted oxidation of 4-tolyl methyl sulfide (**MTS**), selected as a model

substrate. Methanol was employed as the solvent, being generally an optimal medium for the direct and selective oxidation of sulfides [8].

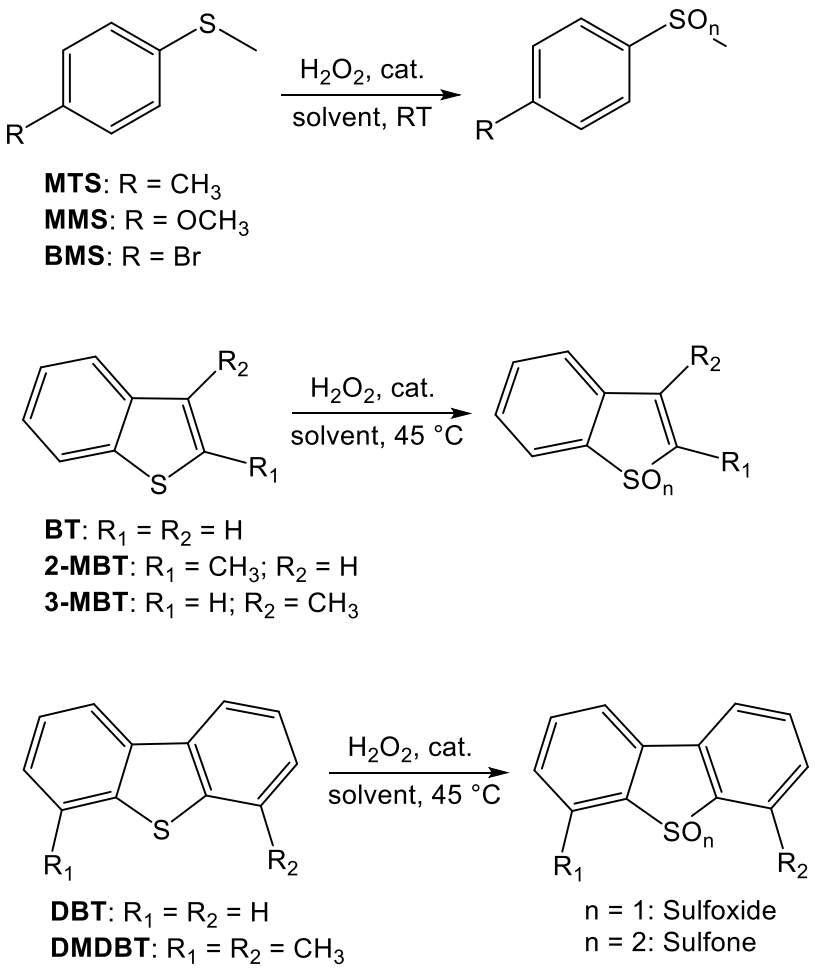

Scheme 1. Overview of sulfides studied in this work and their catalytic H_2O_2 oxidation affording sulfoxide (n = 1) and/or sulfone (n = 2) products.

First, a blank test without catalyst evidenced that the oxidation of **MTS** with 5.0 equiv. of H_2O_2 at room temperature, affording the corresponding sulfoxide as the only product, even after a quite long reaction time (5.0 hours) [27]. The absence of any unproductive decomposition of hydrogen peroxide was confirmed by iodometric titration. The results obtained with catalysts **1**-**5**, under optimized conditions, are shown in Table 1. Both pentacarbamates of Nb (**1**) and Ta (**2**) behaved as efficient catalysts, providing a complete conversion of the starting sulfide in less than 20 minutes, with a comparable higher selectivity

for the formation of the corresponding sulfone. Conversion into the latter was completed after 50 min. (Table 1, entries 1-2). Comparative time-conversion profiles for the oxidation of **MTS** with catalysts **1** and **2** are showed in Figure 2.

Table 1. Comparative catalytic activity for the **MTS** oxidation provided by niobium carbamates (**1**, **3-5**) and [$Ta(O_2CNMe_2)_5$] (**2**).[a]

Entry	Catalyst	MTS (%)[b]	Sulfox. (%)[b]	Sulfone (%)[b]	MTS (%)[b]	Sulfox. (%)[b]	Sulfone (%)[b]	TON[c]
		time = 30 min.			time = 50 min.			
1	**1**	-	20	79	-	-	> 99	100
2	**2**	-	24	75	-	-	> 99	100
3	**3**	29	32	38	7	22	70	93
4	**4**	-	2	97	-	-	> 99	100
5	**5**	80	5	14	64	12	23	36
6[d]	**1**	-	68	31	-	59	40	100
7[d]	**4**	-	25	74	-	10	89	100

[a]Experimental conditions: substrate (0.5 M), MeOH (1.0 mL), catalyst: 1.0 mol % (0.5 mol % for **4**), H_2O_2 (2.0 eq.), RT. [b]Residual amount of substrate (**MTS**) and detected yields of sulfoxide and sulfone, respectively. [c]TON (Turnover number) = mmol of converted substrate/mmol of metal active species. [d]Reaction performed in acetonitrile.

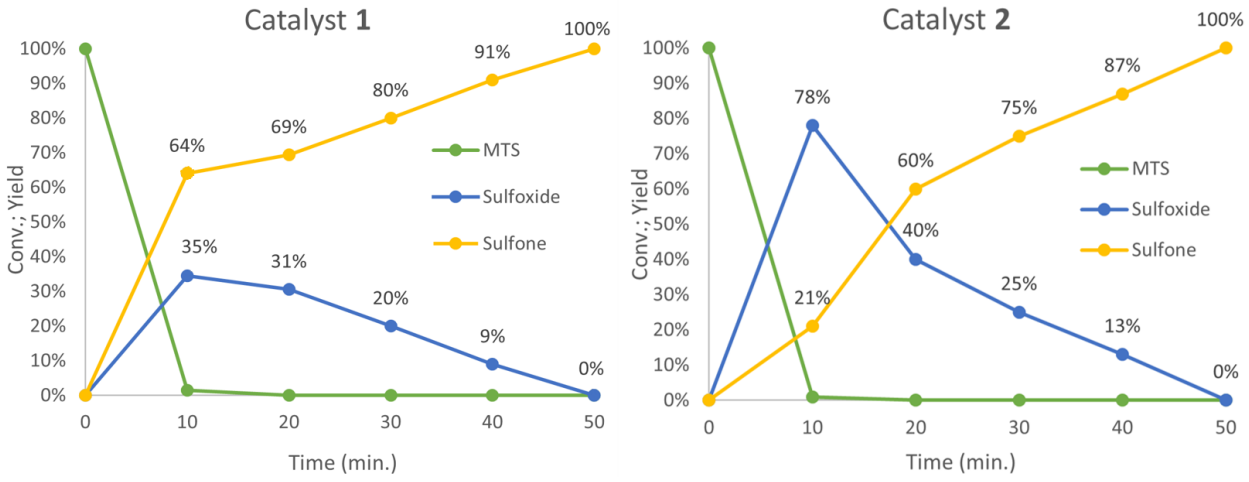

Figure 2. Time-conversion profile for catalytic oxidation of **MTS** with catalysts **1** and **2**. Reaction conditions are reported in Table 1.

Using either **1** or **2** as catalyst, the concentration of the sulfoxide product rapidly increased at the beginning, reaching the maximum value at 10 minutes, and then slowly decreased. The volcano curve observed for the sulfoxide formation with tantalum complex **2** indicates that the sulfoxide is formed as intermediate in larger amount compared to the reaction involving the niobium complex **1**. Besides, the concentration of sulfone increased with time, and more rapidly in the presence of **1**. For the latter catalyst, the sulfone *vs* sulfoxide formation was much faster since the beginning of the reaction. Overall, the oxido-niobium complex **4** showed an excellent activity, affording the corresponding sulfone almost quantitatively after only 30 min. It should be mentioned that the active role exerted by the oxido-metal species in the rapid activation of alkyl-hydroperoxide oxidants, like *tert*-butyl hydroperoxide (TBHP) or the same H_2O_2, has long been recognized for metal complexes of Ti, V, Mo or W, in their highest oxidation state, in various oxygen atom transfer processes [28]. In a different way, we observed that the niobium(IV) carbamate **3** is less active with respect to the niobium(V) complex **1**, the former affording a 70% yield of sulfone after 50 minutes (Table 1, entry 3 vs. entry 1). This result highlights that the oxidation state of niobium may affect the efficiency of the catalytic system [10b]. On the other hand, the hybrid chlorido-carbamato complex **5** displayed a lower activity compared to **1**, in fact prolonging the reaction time till 3.5 hours was required to accomplish the quantitative oxidation of **MTS** to sulfone (Table 1, entry 5). In order to evaluate the possible role of the solvent, we performed the **MTS** oxidation in acetonitrile, working with the two selected niobium complexes **1** and **4**. In both cases, the catalytic activity was lower than in methanol (Table 1, compare entries 6 vs. 1, and entries 7 vs. 4). To reach the quantitative formation of sulfone, 2.5 h time was required for **1**, while 1.5 h was required for **4**. Anyway, **4** confirmed to be the most active catalyst even working in acetonitrile, thus affording 89% of sulfone after only 50 minutes (Table 1, entry 7). In the case of **1**, the acetonitrile medium modified also the selectivity between sulfone and sulfoxide products favouring the latter (Table 1, entries 6 vs. 1). This

difference is presumably ascribable to the influence of methanol on the chemical nature of the catalytic system (see onward), however, the detrimental effect arising from the lower solubility showed in acetonitrile by **2** and **4** should be also taken into account. In our hands, the catalytic oxidation of **MTS** with complex **1**, working under the same conditions of Table 1 but with TBHP (70% aqueous solution) as main oxidant, did not afford satisfying results in comparison with H_2O_2 (less than 40% of substrate conversion after 3.0 hours).

Encouraged by the preliminary results obtained during the catalytic studies performed on **MTS**, we then moved toward the evaluation of the effect of different substituents on the aryl ring of the sulfide reactant, otherwise maintaining the same conditions as those described in Table 1. In detail, we selected, as substrates, 4-methoxyphenyl methyl sulfide (**MMS**) and 4-bromophenyl methyl sulfide (**BMS**), see Scheme 1, containing, respectively, substituents able to increase or reduce the electron density on the sulfur atom (Table 2).

Table 2. Complete catalytic oxidation of **MMS** and **BMS** to the corresponding sulfones by means of carbamato complexes **1-2** and **4-5**.[a]

Entry	**Catalyst**	**Sulfide**[b]	**Time** (h)	**TOF**[c]
1	**1**	**MMS**	1.2	83
2	**1**	**BMS**	4.0	25
3	**2**	**MMS**	0.5	200
4	**2**	**BMS**	2.0	50
5	**4**	**MMS**	1.2	83
6	**4**	**BMS**	4.0	25
7	**5**	**MMS**	2.0	50

[a]Experimental conditions: substrate (0.5 M), MeOH (1.0 mL), catalyst: 1.0 mol % (0.5 mol % for **4**), H_2O_2 (2.0 eq.), RT. [b]Sulfides: MMS = 4-methoxyphenyl methyl sulfide; BMS = 4-bromophenyl methyl sulfide (see Scheme 1). [c]TOF (Turnover frequency) = mmol of converted substrate/(mmol of metal active species · h).

Actually, the electron releasing substituent of **MMS** enhanced the catalytic activity of the tantalum complex **2** with respect to what observed in the **MTS** oxidation, being the complete oxidation to sulfone reached after 30 min. instead of 50 min. (compare Table 2 entry 3 vs. Table 1 entry 2). Also for the niobium hybrid chlorido-carbamato complex **5**, the quantitative formation of sulfone (2 h) was faster for **MMS** (Table 2, entry 7) in comparison with **MTS** (3.5 h). Otherwise, the oxidation of **MMS** was kinetically slightly slower when using the niobium carbamato complexes **1** and **4**, whereby the complete conversion to sulfone was obtained within 70 min. (Table 2, entries 1 and 5), instead of 50 min. (Table 1, entries 1 and 4). The complexes **1**, **2** and **4** were also employed in the catalytic oxidation of **BMS**: the negative effect on the catalytic activity, due to the presence of the electron withdrawing Br-para substituent, was evident in the longer reaction times required for the quantitative oxidation to sulfone (in Table 2, compare entries 2 and 6 vs entries 1 and 5, for catalysts **1** and **4**, respectively). Also with **BMS**, the tantalum pentacarbamate **2** behaved as an active system, affording quantitatively the corresponding sulfone within 2.0 h (Table 2, entry 4).

3.2 Oxidation of aromatic sulfides to corresponding sulfoxides and sulfones.

Aromatic sulfides such as benzothiophene (**BT**) and dibenzothiophene (**DBT**) and their derivatives are a class of hard to oxidize organic sulfur compounds present in high-boiling point petroleum fractions, in particular diesel fuel. Thus, searching for oxidant and catalytic systems ensuring a high degree of oxidative conversion of these compounds is of great importance, especially for what concerns the environmental point of view. As a matter of fact, oxidative desulfurization (ODS) is considered the most promising technology to drastically reduce the sulfur content in fuel [29]. In this process, recalcitrant organosulfur compounds are oxidized to the corresponding sulfoxides and sulfones, which are successively removed by extraction with polar solvents. In the light of the promising results obtained in the oxidation of methyl aryl sulfides, we decided to apply the selected carbamate complexes **1-2** and **4** in the H_2O_2 oxidation of the most challenging aromatic sulfides **BT**, its alkyl substituted derivatives 2-

methyl-1-benzothiophene (**2-MBT**) and 3-methyl-1-benzothiophene (**3-MBT**), and in addition **DBT** and 4,6-dimethyldibenzothiophene (**DMDBT**), see Scheme 1.

Initially, we focused on the evaluation of the performance of **4**, either in methanol or acetonitrile. The moderate reactivity of the aromatic sulfides toward the complete oxidation to sulfones [30], along with the poor solubility showed by **DBT** and **DMDBT** in methanol, prompted us to work under moderate heating (45 °C) with 3.0 equiv. of H_2O_2, otherwise maintaining the conditions described above. As reported in Table 3, very good results in terms of quantitative conversion of substrates and yield of sulfones were obtained in all cases, in a range of time between 2.5 and 6 hours. The observed order of reactivity showed by the different sulfides, namely **BT** > **2-MBT** > **3-MBT** ≈ **DBT** > **DMDBT**, may be rationalized balancing the favourable effect provided by the increase of the electron density on the S atom, with the disadvantageous one caused by the increase of the steric hindrance influencing the accessibility at the same sulfur site [31]. Frequently, in the case of **BT** and **DBT** derivatives, shorter reaction times may be reached by increasing the excess amount of H_2O_2. Newly, the reaction performed in acetonitrile required a longer reaction time, in comparison to methanol, to reach quantitative conversion of the sulfide. In the case of **DMDBT** oxidation, the reaction was only realized in acetonitrile due to the modest solubility of the organic reactant in methanol at 45 °C. In terms of comparative evaluation of the catalytic activity between complexes **1**, **2** and **4**, for the DBT oxidation, the oxido-niobium carbamate **4** showed to be the most active one in all cases. Otherwise, the tantalum derivative **2** revealed the least active catalyst (Table 3, entry 10 vs. entries 7 and 9), although showing a satisfying performance. Finally, the oxidation of **DMDBT** gave good results with both the niobium complexes **1** and **4** (Table 3, entries 12 and 11), on considering that the quantitative yield of sulfone may be obtained by briefly prolonging the reaction time (1-2 hours), the very modest excess of oxidant and the moderate temperature employed.

Unfortunately, attempts to recycle catalyst **4**, by means of extraction of this niobium compound from the reaction medium, led to prevalent decomposition.

Table 3. Quantitative catalytic oxidation of aromatic sulfides with selected carbamate complexes **1-2**, **4**.

Entry	Sulfide	Solvent	Catalyst	Time (h)	Sulfox. (%)[b]	Sulfone (%)[b]	TOF[c]
1	**BT**	MeOH	**4**	2.5	3	96	40
2	**BT**	CH_3CN	**4**	3	2	97	33
3	**2-MBT**	MeOH	**4**	3	-	> 99	33
4	**2-MBT**	CH_3CN	**4**	3.5	10	87	29
5	**3-MBT**	MeOH	**4**	3.5	-	> 99	29
6	**3-MBT**	CH_3CN	**4**	4.0	9	90	25
7	**DBT**	MeOH	**4**	3.5	-	> 99	29
8	**DBT**	CH_3CN	**4**	4.0	-	> 99	25
9	**DBT**	MeOH	**1**	4.0	-	> 99	25
10	**DBT**	MeOH	**2**	5.0	10	88	20
11	**DMDBT**	CH_3CN	**4**	5.5	13	86	18
12	**DMDBT**	CH_3CN	**1**	6.0	18	80	17

[a]Experimental conditions: substrate (0.5 M), catalyst: 1.0 mol % (0.5 mol % for **4**), H_2O_2 (3.0 eq.), 45 °C. [b]Isolated yields of sulfoxide and sulfone. [c]TOF (Turnover frequency) = mmol of converted substrate/(mmol of metal active species · h).

For sake of comparison, a brief outline of the catalytic activity and TOF values of previously described Nb and Ta complexes, in the H_2O_2 promoted oxidation of sulfides, is resumed in Table 4. Accordingly, the relatively high performance of niobium and tantalum carbamates described herein may be inferred, placing them within quite satisfying activity value ranges in comparison to the previously studied catalysts based on different metal species, especially if we concern to ODS processes.[32] Thus, the higher reactivity showed by complexes **4** and **2** toward the complete oxidation of demanding aromatic sulfides like DBT, in comparison with $Nb(OEt)_5$ and $TaCl_5$ (see Table 4, entry 5 vs 4, and entry 7 vs 6), is remarkable. Moreover, as well as other peroxo complexes containing different d^0 metals such as V(V),

Mo(VI) and W(VI), it is worth noting the high catalytic activity of either the preformed peroxo containing Nb(V) complexes, or the ionic liquid stabilized niobium oxoclusters, in the H_2O_2 promoted oxidation of selected sulfides (Table 4, entries 1 and 8 or 2, respectively) [33, 34, 7c].

Table 4. Comparison of catalytic activity of selected Nb and Ta complexes under different reaction conditions.

Entry	Catalyst		Substr.	Oxid./Solv.	Time (h)	Temp. (°C)	Sulfone (Y. %)	TOF[a]	Reference
	Type	Amount							
1	$Nb(O_2)_3L_2$	0.1 mol %	**MTS**	H_2O_2 (2.0 eq.)/H_2O	1.1	RT	97	895	[33]
2	Nb-OC@[TBA][LA]	$2.7 \cdot 10^{-2}$ mol %	**MTS**	H_2O_2 (2.5 eq.)/MeOH	4.0	50	> 99	926	[7c]
3	**4**	0.5 mol%	**MTS**	H_2O_2 (2.0 eq.)/MeOH	0.5	RT	97	200	This work
4	$Nb(OEt)_5$	2 mol %	**DBT**	H_2O_2 (4.0 eq.)/MeOH	3.0	45	98	16.3	[9]
5	**4**	0.5 mol %	**DBT**	H_2O_2 (3.0 eq.)/MeOH	3.5	45	> 99	29	This work
6	$TaCl_5$	10 mol %	**DBT**	H_2O_2 (20 eq.)/MeOH	20	45	98	0.49	[9]
7	**2**	1.0 mol %	**DBT**	H_2O_2 (3.0 eq.)/MeOH	5.0	45	88	20	This work
8	$Nb(O_2)L_2$	$1.25 \cdot 10^{-3}$ mol %	**BT**	H_2O_2 (0.07 eq.)/CH_2Cl_2	7.0	40	52	5943	[34]
9	$Nb(O_2)L_2$	$1.25 \cdot 10^{-3}$ mol %	**DBT**	H_2O_2 (0.07 eq.)/CH_2Cl_2	7.0	70	0	0	[34]
10	**4**	0.5 mol %	**BT**	H_2O_2 (3.0 eq.)/MeOH	2.5	45	96	40	This work

[a]TOF (Turnover frequency) = mmol of converted substrate/(mmol of metal active species · h)

3.3 Mechanistic investigation: NMR and DFT studies

With a view to mechanistic investigations, we selected the oxido-carbamato complex **4** as a promising catalyst, thus we carried out several studies on this compound in order to trace out a possible catalytic cycle. ESI-MS analysis (see Figure S1 in the SI) suggests that **4** turns to be a monomer in solution of methanol from the bottle, then NMR spectroscopy showed that **4** is indefinitely stable under that condition, despite the protic environment including the presence of water. Likewise **4**, also **2** and **3** revealed stable in non-anhydrous methanol solution, whereas NMR analysis on **5** evidenced fast decomposition with formation of diethylamine (consequent to a partial degradation of the carbamato ligands). The minor stability of **5** is presumably ascribable to the presence of Nb^{V}-chlorides, which represent acidic sites favouring the attack by protic species and the consequent rupture of the carbamato moieties [5c,35]. Note that the lower Lewis acidity and activating power of [$NbOCl_3$] towards hard donors, compared to [$NbCl_5$], has been clearly established previously [36].

The solution structure of **4** was investigated by DFT methods. The ethyl groups were replaced by methyl groups to reduce the computational effort of the study, without substantially affecting the electronic and steric factors. The polarity of the methanol was simulated by the conductor-like polarizable continuum (CPCM). The optimized geometries of both the monomeric form, $\mathbf{4}^{\mathbf{mono\text{-}Me}}$, and the dimeric one, $\mathbf{4}^{\mathbf{dimer\text{-}Me}}$, were calculated (Figure 3). The enthalpy and Gibbs free energy differences ongoing from $\mathbf{4}^{\mathbf{mono\text{-}Me}}$ to $\mathbf{4}^{\mathbf{dimer\text{-}Me}}$ are -17.2 and 1.7 kcal/mol, respectively: this means that the monomer is slightly more stable than the dimer in methanol solution, in agreement with the ESI-MS outcome, essentially due to the entropic cost of the dimerization. Given the small value of ΔG, the dimer (which represents the stable species in the solid state, see Figure 1) is still accessible in solution.

The structure of $\mathbf{4}^{\mathbf{mono\text{-}Me}}$ (Figure 3A) shows that the Nb=O bond is 1.731 Å long and all the carbamate ligands are asymmetrically κ^2-O,O coordinated to the metal centre, with two of them lying on the equatorial plane (Nb-O distances 2.136 and 2.191 Å), and the third one occupying the axial position *trans* to the oxide (Nb-O = 2.362 Å) and the remaining equatorial position (Nb-O = 2.104 Å). The *trans* effect of the oxide induces a relevant weakening of the axial Nb-O bond. This bond is so loose that, in solution,

the related carbamate may turn to monodentate, and the vacant site occupied by a molecule of solvent, if sufficiently coordinating (e.g., methanol or acetonitrile). Furthermore, the same site is susceptible to attack by a second molecule of **4**$^{\text{mono-Me}}$, giving back the dimer (Figure 3B, compare to Figure 1). In **4**$^{\text{dimer-Me}}$, the Nb-O distances remain similar, with two carbamates bridging the two metals.

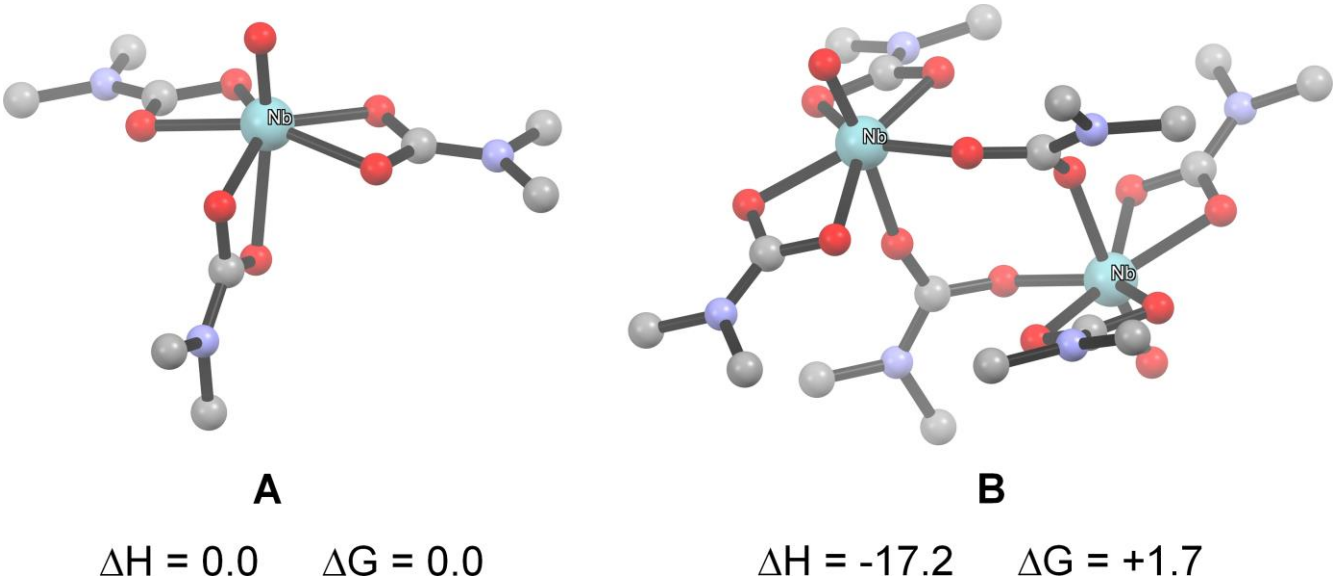

Figure 3. Views of the DFT-optimized geometries of **4**$^{\text{mono-Me}}$ (**A**) and **4**$^{\text{dimer-Me}}$ (**B**). H atoms omitted for clarity. Thermodynamic parameters are given in parentheses (kcal/mol) and are relative to complex **A**, chosen as an arbitrary energy reference.

When an excess of H_2O_2 (up to 150 equivalents) was added to the CD_3OD solution of **4**, decomposition occurred to a minor degree (ca. 15%). In fact, N-ethylideneethanamine oxide, Me(H)C=N(Et)O, was identified in the solution, reasonably generated by degradation of a fraction of carbamato ligands (approximately, 1:6), triggered by subsequent H_2O_2 oxidation of the released amine [37]. The NMR signals related to the carbamato moieties in the mixture were almost coincident with those ones of the starting complex **4** (Figures S5-S7), and no additional signals were found. This picture suggests that a fast equilibrium between **4** (major) and the *in situ* generated mono-methoxide derivative $[NbO(OCD_3)(O_2CNEt_2)_2]$, **6** (minor), takes place.

Unfortunately, low temperature NMR and mass spectrometry analyses were not conclusive to confirm this hypothesis that, however, seems plausible. A similar decomposition pattern was detected with **2** and **3**.

The substantial robustness exhibited by **2-4** even in the presence of hydrogen peroxide/water is a surprising feature since metal carbamates are known to be reactive towards protic species and routinely stored under inert atmosphere to prevent rapid degradation in contact with air moisture (see Introduction) [13,38].

When Me_2S (as a model sulfide) was added to the solution containing **4**, quantitative conversion into Me_2SO_2 was NMR detected, the signals related to the niobium compound being unchanged. Further NMR experiments pointed out that neither Me_2S nor Me_2SO enters the coordination sphere of **4**, and that Me_2S oxidation by means of H_2O_2 stops at the formation of Me_2SO in the absence of **4** (see Figure S9-S12). In alignment with the major activity furnished by **4** in the catalytic experiments, only a partial conversion of Me_2S into Me_2SO_2 was detected using **2** or **3** in the place of **4**. Furthermore, we repeated the catalytic oxidation of **MTS** with H_2O_2, in the presence of **4** and a stoichiometric amount of a radical scavenger, i.e. 2,6-di-*tert*-butyl-4-methylphenol (BHT), otherwise using the conditions reported in Table 1: the result is well comparable with that one achieved in the absence of BHT. Overall, the experimental findings indicate **4** as a probable catalytic species involved in the related sulfide oxidation reactions, and that no radicals are involved in the catalytic cycle, as previously established for other niobium-catalysed processes [39]. Based on these observations, we carried out a computational study (Scheme 2). First, an adduct (**RC**) between the mononuclear, methyl-analogue of **4**, i.e. $\mathbf{4^{mono\text{-}Me}}$, and H_2O_2 was optimized, wherein two hydrogen bonds are established between the protons of H_2O_2 and the oxygen atoms of the carbamates. The enthalpy for the formation of **RC** is negative (-6.3 kcal/mol) but the Gibbs free energy is positive (+7.2 kcal/mol). Then, the oxide can abstract a proton from H_2O_2, assisting the coordination of the hydroperoxyl moiety to the metal. The two steps are concerted in **TS1** ($\Delta H^{\ddagger}$ = 7.9 kcal/mol, $\Delta G^{\ddagger}$ = 23.7 kcal/mol), leading to **Int1**, where the carbamates are still present as bidentate donors and hydroxyl

and hydroperoxyl groups coordinate the niobium in mutual cis position (ΔH = -3.5 kcal/mol, ΔG = 9.8 kcal/mol) [40].

The possible and alternative formation, *in situ*, of hydroxyperoxoniobate species $[L_3Nb(OH)(\eta^2\text{-}O_2)]^-$ following H_2O_2 addition, should be ruled out, since the energy barrier for the following oxygen transfer reaction toward sulfide is *ca.* 9 kcal/mol lower for $[L_3Nb(OH)OOH]$ (**Int1**, Scheme 2) than for $[L_3Nb(OH)(\eta^2\text{-}O_2)]^-$ [41].

The intermediate **Int1** forms an adduct with SMe_2 (**Int2**, ΔH = -10.3 kcal/mol, ΔG = 16.0 kcal/mol) through a hydrogen bond between the sulfur and the hydroxyl group. This system evolves with an intramolecular attack of the sulfur to one oxygen of the hydroperoxyl group. Attack to the metal-bound oxygen did not lead to any transition state or stable product, whereas attack to the distal oxygen led to a reasonable TS (**TS2**, $\Delta H^{\ddagger}$ = -1.4 kcal/mol, $\Delta G^{\ddagger}$ = 24.2 kcal/mol). It is interesting to note that the OÔS angle is 171.9°, quite close to 180°, whereas the OŜC angle is 96.1° (Figure S13 and Scheme 2). This suggests that the sulphur attacks the oxygen by one of its lone pair. Then, the proton migration from the incipient species Me_2SOH^+ to Nb-O^- is barrierless, causing the release of Me_2SO. The resulting intermediate **Int3** bears two hydroxyl groups on the metal (ΔH = -43.7 kcal/mol, ΔG = -30.0 kcal/mol). Subsequently, these two –OH groups can interact with each other, to form water (**TS3**, $\Delta H^{\ddagger}$ = -40.1 kcal/mol, $\Delta G^{\ddagger}$ = -26.8 kcal/mol) and regenerate $\mathbf{4^{mono\text{-}Me}}$. The global activation energy for the catalytic cycle depicted in Scheme 2 is 24.2 kcal/mol, which is a reasonable value for a room temperature catalytic process.

Regarding the $SOMe_2/SO_2Me_2$ oxidation step, it is expected that it has a higher activation barrier, as the lone pair of the sulphur is likely less nucleophilic in $SOMe_2$, due to the electron-withdrawing effect of the oxygen. As a confirmation, the DFT-computed activation barrier ($\Delta G^{\ddagger}$) is 28.8 kcal/mol (**2nd_TS2** structure, see Supporting Information), still feasible but higher than that of $SMe_2/SOMe_2$ oxidation. This is in agreement with Figure 2, which shows that the $SMe_2/SOMe_2$ oxidation is very fast and already

complete in some minutes, whereas the subsequent $SOMe_2/SO_2Me_2$ step is slower and requires almost one hour.

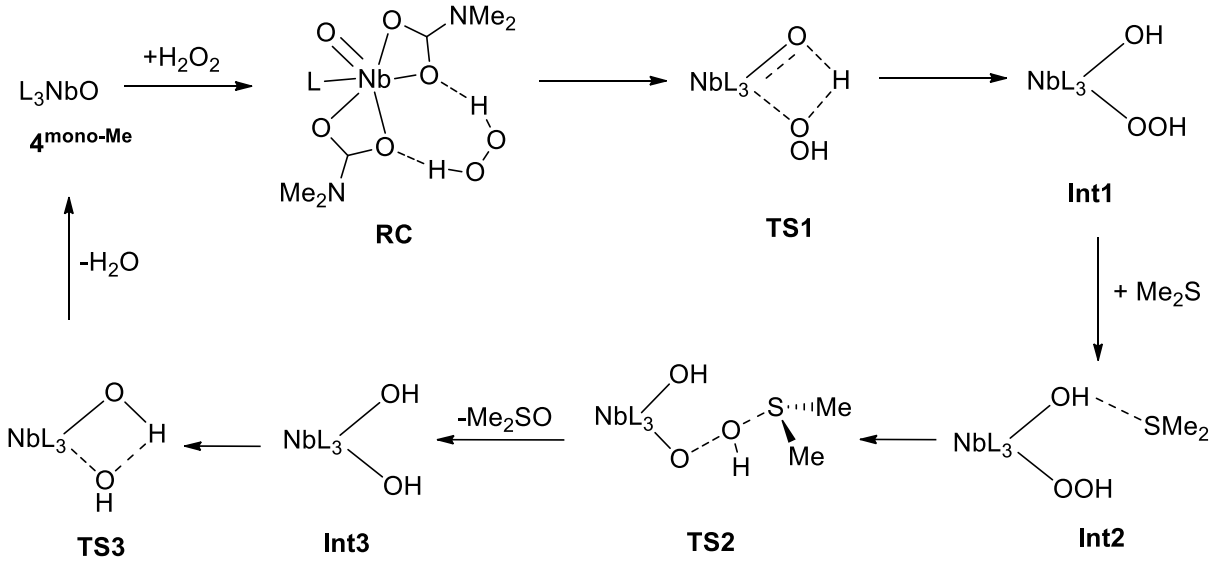

Scheme 2. Proposed mechanism for the dimethylsulfide oxidation catalysed by niobium(V) oxido tris-carbamate (L = $OOCNMe_2$ or OMe).

For the sulfoxide/sulfone conversion, the mechanism is most likely similar to that discussed for the sulfide/sulfoxide oxidation (Scheme 2). Anyway, the lone pair of the sulfoxide is expected to be less nucleophile than that of the sulfide, because of the electron-withdrawing effect of the oxygen, leading to a higher activation barrier for **TS2** (Scheme 2). This would explain why the second oxidation step is slower than the first one, as suggested by Figure 2. However, considering that **4** is not the only niobium compound present in the reaction environment (see above), we investigated by DFT the possible solvolysis of the model compound $\mathbf{4}^{\mathbf{mono\text{-}Me}}$ to the methoxy-derivative $\mathbf{6}^{\mathbf{mono\text{-}Me}}$ (Scheme 3). The consequent oxidation of the released dimethylamine to CH_2=N(Me)O, water and dihydrogen gas make the global reaction very favoured both in terms of enthalpy (ΔH_r = -20.5 kcal/mol) and Gibbs free energy (ΔG_r = -1.9 kcal/mol).

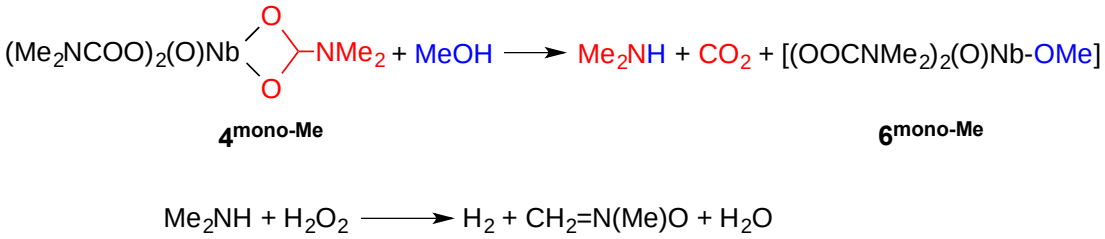

Scheme 3. Methanolysis of one carbamato unit belonging to niobium(V) oxido tris-carbamate, according to NMR evidence, and subsequent amine oxidation by hydrogen peroxide.

The catalytic performance of $\mathbf{6}^{\mathbf{mono\text{-}Me}}$ was also computationally explored, analysing the same steps established for $\mathbf{4}^{\mathbf{mono\text{-}Me}}$ (Scheme 2); here, the activation barrier ($\Delta G^{\ddagger}$) is 16.8 kcal/mol (relative to **TS1bis**: red line in Figure S14), therefore lower than in the case of $\mathbf{4}^{\mathbf{mono\text{-}Me}}$ (23.7 kcal/mol). Briefly, the ethyl analogues of both $\mathbf{4}^{\mathbf{mono\text{-}Me}}$ and $\mathbf{6}^{\mathbf{mono\text{-}Me}}$ reasonably act as catalysts in the oxidation reactions involving **4**. It is possible that the two niobium structures, i.e. $\mathbf{4}^{\mathbf{mono\text{-}Me}}$ and $\mathbf{6}^{\mathbf{mono\text{-}Me}}$ (and, consequently, their ethyl analogues which have been experimentally employed), exist in solution in equilibrium with each other through an associative mechanism. The geometry of the resulting mixed dimer ($\mathbf{4\_6}^{\mathbf{Me}}$) was optimized (Figure S15). Its structure and bond lengths are quite similar to those of $\mathbf{4}^{\mathbf{dimer\text{-}Me}}$, with the obvious difference that one carbamate is replaced with a methoxy moiety. The adduct $\mathbf{4\_6}^{\mathbf{Me}}$ is slightly less stable than the sum of the isolated components (ΔH = -16.1 kcal/mol, ΔG = 2.9 kcal/mol). During the dissociation, the exchange of carbamato ligands presumably occurs, thus explaining the fast equilibrium and, consequently, the presence of only one set of NMR resonances. Note that relevant examples of fast intermolecular exchange of carbamato ligands, between transition metal centres, were previously reported in the literature [**Error! Bookmark not defined.**,42].

Finally, as the catalytic system contains also water and the molecular systems discussed here contain either acidic and basic sites, the effect of hydrogen-bonded molecules of water on the energy levels shown in Figure S14, has been tested. In particular, the adduct $\mathbf{6}^{\mathbf{mono\text{-}Me}}$-$H_2O$ has been optimized. Even if the formation enthalpy of the adduct is negative (-3.1 kcal/mol), the entropic cost makes the formation

Gibbs energy positive (+6.6 kcal/mol), thus making these hydrogen bonded adducts kinetically unimportant in the mechanism.

4. Conclusions

The oxidation of sulfides is a challenging reaction with important industrial implications, and the development of new and effective metal catalysts able to promote the selective conversion up to sulfones has aroused a notable attention. In this specific research field, beside the largely explored activity of various vanadium complexes, only a few studies have regarded high valent niobium and tantalum complexes. Metal carbamates constitute a wide class of compounds which are easily available from inexpensive materials and for which the exploration of the catalytic potential has been limited by the "dogma" predicting facile degradation of the carbamato moiety in protic environments. The development of metal carbamates for catalytic applications is valuable due to their simplicity and cost effectivenessm the versatility and peculiar chemical behavior of the carbamato ligand, and the synthesis reaction involving the capture of carbon dioxide under ambient conditions. Here, we have found that a selection of high valent niobium and tantalum compounds are efficient catalytic precursors to convert a series of sulfides into the corresponding sulfones under mild conditions. In particular, niobium(V) oxido tris-carbamate **4** emerged as a really efficient catalyst, related to the unexpected robustness of this complex in methanol/water/H_2O_2 ambient. Remarkably, the activity exhibited by niobium and tantalum carbamates in the conversion of aromatic sulfides into the corresponding sulfones exceeds that previously reported for the other high valent niobium and tantalum species [9], while the performance in the oxidation of linear alkyl aryl sulfides parallels that provided by the best high valent niobium and tantalum derivatives in the literature.

Compound **4** was selected as a model to trace a plausible catalytic cycle. A joint DFT and NMR study reveals the presumable existence of two interconverting species catalytically active in the reaction medium, *i.e.* the starting complex and its mono-methoxide derivative. The mechanistic features confirm

the ability of high valent niobium derivatives to efficiently generate hydroxyl hydroperoxy reactive species upon contact with hydrogen peroxide [33], and outline the versatile role of the carbamato units, capable of readily switching from bidentate to monodentate and viceversa. These results encourage further progress in the in-depth assessment of the catalytic properties of valuable metal carbamates.

***Corresponding Authors**

E-mail addresses: gianluca.ciancaleoni@unipi.it (G.C.); fabio.marchetti1974@unipi.it (F.M.); marcello.crucianelli@univaq.it (M.C.)

Acknowledgements

We gratefully thank the Universities of Pisa (PRA_2020_39) and L'Aquila (RIA 2020) for financial support.

Supporting Information Available

ESI-MS spectrum of complex **4** in methanol; IR and NMR studies; selected GC-MS and NMR spectra of sulfones; further details on DFT study along with views of DFT-optimized geometries and Cartesian coordinates of the DFT structures.

References

1 a) S. Patai, Z. Rappoport (Eds), Synthesis of Sulfones, Sulfoxides and Cyclic Sulfides, J. Wiley, Chichester (1994). (b) I. Fernandez, N. Khiar, Chem. Rev. 103 (2003) 3651–3706. (c) M. Feng, B. Tang, S. H. Liang, X. Jiang, Curr. Top. Med. Chem. 16 (2016) 1200–1216. (d) J. Legros, J. R. Dehli, C. Bolm, Adv. Synth. Catal. 347 (2005) 19–31

2 (a) F. Carniato, C. Bisio, R. Psaro, L. Marchese, M. Guidotti, Angew. Chem. Int. Ed. 53 (2014) 10095–10098. (b) J. Dong, J. Hu, Y. Chi, Z. Lin, B. Zou, S. Yang, C. L. Hill, C. Hu, Angew. Chem. Int. Ed. 56 (2017) 4473–4477

3 A. Rajendran, T.-y. Cui, H.-x. Fan, Z.-f. Yang, J. Feng, W.-y. Li, J. Mater. Chem. A 8 (2020)0 2246–2285.

4 Selected references: (a) R. R. Langeslay, D. M. Kaphan, C. L. Marshall, P. C. Stair, A. P. Sattelberger, M. Delferro, Chem. Rev. 119 (2019) 2128−2191. (b) V. Conte, B. Floris, Inorg. Chim. Acta 363 (2010) 1935–1946. (c) N. Hall, M. Orio, A. Jorge-Robin, B. Gennaro, C. Marchi-Delapierre, C. Duboc, Inorg. Chem. 52 (2013) 13424-13431. (d) H. Pellissier, Coord. Chem. Rev. 284 (2015) 93–110. (e) A. S. Ogunlaja, W. Chidawanyika, E. Antunes, M. A. Fernandes, T. Nyokong, N. Torto, Z. R. Tshentu, Dalton Trans. 41 (2012) 13908–13918. (f) P. Campitelli, M. Aschi, C. Di Nicola, F. Marchetti, R. Pettinari, M. Crucianelli, Appl. Cat. A 599 (2020) 117622.

5 (a) Y. Satoh, Y. Obora, Eur. J. Org. Chem. (2015) 5041–5054. (b) A. M. Raspolli Galletti, G. Pampaloni, Coord. Chem. Rev. 254 (2010) 525-536. (c) F. Marchetti, G. Pampaloni, Chem. Commun. 48 (2012) 635–653.

6 (a) H. Egami, T. Oguma, T. Katsuki, J. Am. Chem. Soc. 132 (2010) 5886–5895.
(b) C. Leal Marchena, G. Gina, L. Pierella, Mol. Catal. 482 (2020) 110685.

7 (a) M. Kirihara, S. Suzuki, N. Ishihara, K. Yamazaki, T. Akiyama, Y. Ishizuka, Synthesis 49 (2017) 2009–2014. (b) E. V. Rakhmanov, Dan Jinyuan, O. A. Fedorova, A. V. Tarakanova, A. V. Anisimov, Petroleum Chem. 51 (2011) 216–221. (c) Q. Zhou, M. Ye, W. Ma, D. Li, B. Ding, M. Chen, Y. Yao, X. Gong, Z. Hou, Chem. Eur. J. 25 (2019) 4206 – 4217.

8 M. Kirihara, J. Yamamoto, T. Noguchi, Y. Hirai, Tetrahedron Letters 50 (2009) 1180–1183.

9 M. Kirihara, J. Yamamoto, T. Noguchi, A. Itou, S. Naito, Y. Hirai, Tetrahedron 65 (2009) 10477–10484,

10 Selected reviews: (a) M. Olga Guerrero-Pérez, Catal. Today 354 (2020) 19-25; (b) M. Ziolek, I. Sobczak. Catal. Today 285 (2017) 211–225. (c) D. Bayot, M. Devillers, Coord. Chem. Rev. 250 (2006) 2610–2626; (d) I. Nowak, M. Ziolek. Chem. Rev. 99 (1999) 3603-3624.

11 See, for instance (a) P. F. Gostin, A. Helth, A. Voss, R. Sueptitz, M. Calin, J. Eckert, A. Gebert, J. Biomed. Mater. Res. 101B (2013) 269-278. (b) I. Jirka, M. Vandovcova, O. Frank, Z. Tolde, J. Plsek, T. Luxbacher, L. Bacakova, V. Stary, Mater. Sci. Eng. C33 (2013) 1636-1645. (c) M. Niinomi, M. Nakai, J. Hieda, Acta Biomater. 8 (2012) 3888-3903.

12 (a) C. W. Jones, Application of Hydrogen Peroxide and Derivatives, Royal Society of Chemistry, Cambridge (1999). (b) G. Strukul, A. Scarso, M.G. Clerici, O.A. Kholdeeva (Eds.), Liquid Phase Oxidation via Heterogeneous Catalysis: Organic Synthesis and Industrial Applications, Wiley, Hoboken (2013) pp. 1–20 Ch. 1. (c) J.M. Campos-Martin, G. Blanco-Brieva, J.L.G. Fierro, Angew. Chem. Int. Ed. 45 (2006) 6962–6984

13 D. Belli Dell'Amico, F. Calderazzo, L. Labella, F. Marchetti, G. Pampaloni, Chem. Rev. 103 (2003) 3857-3898.

14 L. Biancalana, G. Bresciani, C. Chiappe, F. Marchetti, G. Pampaloni, C. S. Pomelli, Phys. Chem. Chem. Phys. 20 (2018) 5057--5066.

15 D. Belli Dell'Amico, F. Calderazzo, U. Englert, L. Labella, F. Marchetti, M. Specos, Eur. J. Inorg. Chem. (2004) 3938-3945.

16 (a) F. Marchetti, G. Pampaloni, Y. Patil, A. M. Raspolli Galletti, F. Renili, S. Zacchini, Organometallics 30 (2011) 1682-1688; (b) C. Forte, M. Hayatifar, G. Pampaloni, A. M. Raspolli Galletti, F. Renili, S. Zacchini, J. Polym. Sci. Part A: Polym. Chem. 49 (2011) 3338-3345.

17 F. Marchetti, G. Pampaloni, C. Pinzino, F. Renili, T. Repo, S. Vuorinen, Dalton Trans. 42 (2013) 2792-2802.

18 (a) G. Bresciani, M. Bortoluzzi, F. Marchetti, G. Pampaloni, ChemSusChem 11 (2018) 2737-2743. (b) G. Bresciani, F. Marchetti, G. Rizzi, A. Gabbani, F. Pineider, G. Pampaloni, J. CO_2 Utilization 28 (2018) 168–173. (c) G. Bresciani, F. Marchetti, G. Pampaloni, New J. Chem. 43 (2019) 10821-10825. (d) G. Bresciani, M. Bortoluzzi, C. Ghelarducci, F. Marchetti, G. Pampaloni, New J. Chem. 45 (2021) 4340.

19 G. Bresciani, S. Zacchini, F. Marchetti, G. Pampaloni, Dalton Trans. 50 (2021) 5351-5359.

20 M. Hayatifar, C. Forte, G. Pampaloni, Y. V. Kissin, A. M. Raspolli Galletti, S. Zacchini, J. Polym. Sci. 51 (2013) 4095-4102.

21 M. Bortoluzzi, G. Bresciani, F. Marchetti, G. Pampaloni, S. Zacchini, New J. Chem. 41 (2017) 1781-1789.

22 G. R. Fulmer, A. J. M. Miller, N. H. Sherden, H. E. Gottlieb, A. Nudelman, B. M. Stoltz, J. E. Bercaw, K. I. Goldberg, Organometallics 29 (2010) 2176-2179.

23 P. B. Arimondo, F. Calderazzo, U. Englert, C. Maichle-Moessmer, G. Pampaloni, J. Straehle, J. Chem. Soc., Dalton Trans. (1996) 311–319.

24 M. Bortoluzzi, F. Ghini, M. Hayatifar, F. Marchetti, G. Pampaloni, S. Zacchini, Eur. J. Inorg. Chem. (2013) 3112–3118.

25 F. Neese, Wiley Interdiscip. Rev. Comput. Mol. Sci. 8 (2017) e1327.

26 S. Grimme, J. Antony, S. Ehrlich, H. Krieg, J. Chem. Phys. 132 (2010) 154104.

27 F. Shi, M. K. Tse, H. M. Kaiser, M. Beller, Adv. Synth. Catal. 349 (2007) 2425-2430.

28 R. A. Sheldon, J. Mol. Catal. 20 (1983) 1-26.

29 (a) Z. Ismagilov, S. Yashnik, M. Kerzhentsev, V. Parman, A. Bourane, F. M. Al-Shahrani, A.A. Haji, O. R. Koseoglu, Oxidative desulfurization of hydrocarbon fuels. Catal. Rev. Sci. Eng. 53 (2011) 199–255; (b) L. C.A. de Oliveira, N. T. Costa, J. R. Pliego Jr, A. C. Silva, P. P. de Souza, P. S. de O. Patrício, Appl. Catal. B 147 (2014) 43-48.

30 (a) J. L. García-Gutiérrez, G. A. Fuentes, M. E. Hernández-Terán, P. García, F. Murrieta-Guevara, F. Jiménez-Cruz, Appl. Catal. A 334 (2008) 366–373; (b) A. Di Giuseppe, M. Crucianelli, F. De Angelis, C. Crestini, R. Saladino, Appl. Catal. B: Environmental 89 (2009) 239–245.

31 (a) H. Lü, C. Deng, W. Ren, X. Yang, Fuel Process. Technol. 119 (2014) 87–91; (b) W. Zhu, W. Huang, H. Li, M. Zhang, W. Jiang, G. Chen, C. Han, Fuel Proc. Technol. 92 (2011) 1842–1848; (c) S. Otsuki, T. Nonaka, N. Takashima, W. Qian, A. Ishihara, T. Imai, T. Kabe, Energy Fuels 14 (2000) 1232–1239.

32 (a) A. Rajendran, T.-y. Cui, H.-x. Fan, Z.-f. Yang, J. Feng, W.-y. Li, J. Mater. Chem. A 8 (2020) 2246–2285; (b) D. Piccinino, I. Abdalghani, G. Botta, M. Crucianelli, M. Passacantando, M. L. Di Vacri, R. Saladino, Appl. Cat. B 200 (2017) 392–401.

33 S. R. Gogoi, J. J. Boruah, G. Sengupta, G. Saikia, K. Ahmed, K. K. Bania, N. S. Islam, Catal. Sci. Technol., 5 (2015) 595–610.

34 Tkhai Fam Vin', A. V. Tarakanova, O. V. Kostyuchenko, B. N. Tarasevich, N. S. Kulikov, A. V. Anisimov, Theoretical Foundations of Chemical Engineering 42 (2008) 636–642.

35 M. Bortoluzzi, M. Hayatifar, F. Marchetti, G. Pampaloni, S. Zacchini, Inorg. Chem. 54 (2015) 4047−4055

36 N. Bartalucci, M. Bortoluzzi, G. Pampaloni, C. Pinzino, S. Zacchini, F. Marchetti, Dalton Trans. 47 (2018) 3346–3355.

37 (a) S. Murahashi, T. Shiota, Tetrahedron Letters 21 (1987) 2383-2386. (b) R. Joseph, A. Sudalai, T. Ravindranathan 11 (1995) 1177- 1178. (c) M. Colladon, A. Scarso, G. Strukul, Green Chem. 10 (2008) 793-798.

38 G. Bresciani, L. Biancalana, G. Pampaloni, F. Marchetti, Molecules 25 (2020) 3603.

39 N. E. Thornburg, A. B. Thompson, J. M. Notestein, ACS Catal. 5 (2015) 5077−5088.

40 I. D. Ivanchikova, I. Y. Skobelev, N. V. Maksimchuk, E. A. Paukshtis, M. V. Shashkov, O. A. Kholdeeva, J. Catal. 356 (2017) 85–99.

41 N. Antonova, J.J. Carbó, U. Kortz, O.A. Kholdeeva, J.M. Poblet, J. Am. Chem. Soc. 132 (2010) 7488–7497

42 (a) F. Calderazzo, G. Pampaloni, M. Sperrle, U. Englert, Z. Naturforsch. B 47 (1992) 389–394. (b) C. Forte, G. Pampaloni, C. Pinzino, F. Renili, Inorg. Chim. Acta 365 (2011) 251–255. (c) M. H. Chisholm, M. W. Extine, J. Am. Chem. Soc. 99 (1977) 792–802. (d) M. H. Chisholm, M. W. Extine, J. Am. Chem. Soc. 99 (1977) 782–792. (e) D. Belli Dell'Amico, F. Calderazzo, U. Giurlani, G. Pelizzi, Chem. Ber. 6 (1987) 955–964. (f) D. Belli Dell'Amico, F. Calderazzo, F. Gingl, L. Labella, J. Straehle, Gazz. Chim. Ital. 124 (1994) 375–380. (g) P. B. Arimondo, F. Calderazzo, R. Hiemeyer, C. Maichle-Mössmer, F. Marchetti, G. Pampaloni, J. Strähle, Inorg. Chem. 37 (1998) 5507–5511.